Extensive Theoretical Studies on the Low-Lying Electronic States of Indium Monochloride Cation, $InCl^+$

WENLI ZOU, WENJIAN LIU

Institute of Theoretical and Computational Chemistry, and State Key Laboratory of Rare Earth Materials Chemistry and Applications, College of Chemistry and Molecular Engineering, Peking University, Beijing 100871, People's Republic of China

Received 7 May 2004; Accepted 29 July 2004
DOI 10.1002/jcc.20126
Published online in Wiley InterScience (www.interscience.wiley.com).

Abstract: The global potential energy curves for the 14 low-lying doublet and quartet Λ-S states of $InCl^+$ are calculated at the scalar relativistic MR-CISD+Q (multireference configuration interaction with single and double excitations, and Davidson's correction) level of theory. Spin-orbit coupling is accounted for via the state interaction approach with the full Breit–Pauli Hamiltonian, which leads to 30 Ω states. The computed spectroscopic constants of nine bound Λ-S states and 17 bound Ω states are in good agreement with the available experimental data. The transition dipole moments and Franck–Condon factors of selected transitions are also calculated, from which the corresponding radiative lifetimes are derived.

 J Comput Chem 26: 106–113, 2005

Key words: excited states; potential energy curves; spectroscopic constants; spin-orbit coupling; MR-CISD+Q

Introduction

The monohalides of the Ga and In atoms play important roles in the development of high-frequency semiconductor devices and opto-electronic applications.[1,2] Therefore, the detailed interpretation of their electronic and molecular structures deserves great attention. The low-lying electronic states of the InCl molecule have recently been summarized and theoretically studied by Zou et al.[3] However, only a few experiments have heretofore focused on its cation, $InCl^+$. The first experimental investigation on $InCl^+$ was carried out by Berkowitz and Dehmer[4] using He(I) photoelectron spectroscopy. They observed three states ($X^2\Sigma^+$, $A^2\Pi$, and $B^2\Sigma^+$) of $InCl^+$ and reported both the adiabatic and vertical ionization potentials of InCl. More accurate He(I) and He(II) photoelectron spectra of $InCl^+$ were reported by Egdell and Orchard[5] a few years later. A high-resolution emission spectrum of the $B^2\Sigma^+ \rightarrow X^2\Sigma^+$ transition of $InCl^+$ was then recorded by Balfour and his coworkers.[6,7] They got the Rydberg–Klein–Rees (RKR) potential energy curves (PECs), spectroscopic constants, and Franck–Condon factors. Some weak bands between 320 and 335 nm were also obtained. In 1988, a new $C^2\Pi$ state with two Ω components of 1/2 and 3/2 was observed by Glenewinkel–Meyer et al.,[8] and an unobserved $D^2\Sigma^+$ state was also suggested. Moreover, two band systems in the regions of 390–410 and 246–251 nm, which were once regarded as the spectra of the InCl molecule,[9,10] were pointed out to be the transitions $B^2\Sigma^+_{1/2} - X^2\Sigma^+_{1/2}$,[7] and $C^2\Pi_{3/2} - X^2\Sigma^+_{1/2}$ of $InCl^+$, respectively.[3]

The low-lying electronic states of some IIIA group cationic monohalides, such as BBr^+,[11] AlF^+,[12] $AlCl^+$,[12] GaF^+,[13] and $GaCl^+$,[13] have been extensively investigated theoretically. In contrast, so far the only theoretical study on $InCl^+$ was due to Schwerdtfeger et al.[14] They reported the spectroscopic constants of the ground state at various levels of theory. To the best of our knowledge, there have been no theoretical investigations on the excited states of $InCl^+$.

In this contribution we have performed *ab initio* all-electron relativistic calculations for the ground and low-lying excited states of $InCl^+$. The spectroscopic constants and radiative lifetimes are reported for the first time.

Computational Details

All calculations are performed with the MOLPRO 2002.7 program package.[15] A set of $20s16p11d2f$ Gaussian-type functions is used for In, which is obtained by augmenting the set of $20s16p11d1f$[16] with one *f*-function (0.60868955). The standard aug-cc-pVTZ

Correspondence to: W. Liu; e-mail: liuwj@pku.edu.cn

Contract/grant sponsor: National Natural Science Foundation of China; contract/grant numbers: 20243001, 20273004, and 20333020

Contract/grant sponsor: Scientific Research Foundation for the Returned Overseas Chinese Scholars, State Education Ministry of China

Table 1. Relations between Λ-S States and Ω States of $InCl^+$.

Λ-S states	$\|S_z\| = 1/2$	$\|S_z\| = 3/2$
$^2\Sigma^+$ and $^2\Sigma^-$	1/2	
$^2\Pi$	3/2, 1/2	
$^2\Delta$	5/2, 3/2	
$^4\Sigma^+$ and $^4\Sigma^-$	1/2	3/2
$^4\Pi$	3/2, 1/2	5/2, 1/2
$^4\Delta$	5/2, 3/2	7/2, 1/2

(augmented correlation consistent polarized valence triple zeta) basis set[17] is used for Cl. Both sets are uncontracted in the calculations. Scalar relativistic effects are taken into account variationally via the second-order one-electron Douglas–Kroll–Hess (DKH) approach,[18,19] whereas spin-orbit coupling is treated via the state interaction approach with the full Breit–Pauli Hamiltonian (H_{BP}).[20]

Because a number of states of different characteristics in the wave functions will be considered simultaneously, it is important to generate *balanced* orbitals for use in subsequent correlation calculations. For this, state-averaged MCSCF (multiconfiguration self-consistent field) calculations are performed to guarantee the required degeneracy of the relevant states. The active space consists of eight molecular orbitals and nine electrons resulting from the In $5s5p$ and Cl $3s3p$ shells. The $4d^{10}$ electrons of In are always doubly occupied, while the rest of the electrons are kept frozen. As for the treatment of dynamical electron correlation, the internally contracted MR-CISD+Q (multireference configuration interaction with singles and doubles, and Davidson's correction) is used. This is also the highest level of theory available in MOLPRO to combine electron correlation with spin-orbit coupling.

All the calculations are carried out in the C_{2v} subgroup of $C_{\infty v}$. In the C_{2v} double-group symmetry, all the spinors ($\Omega = 1/2$, 3/2, 5/2, and 7/2) of $InCl^+$ are transformed as the $E_{1/2}$ irreducible representation. Nonetheless, these data can be mapped back to the $C_{\infty v}$ double-group symmetry by identifying the projection of the spin angular momentum on the z-axis ($|S_z|$) (cf. Table 1) as well as the mixtures between these half-integral spinors. The PECs are then obtained by connecting the calculated energy points with the aid of the avoided-crossing rule between electronic states of the same irreducible representation of the $C_{\infty v}$ double group.

From the PECs of the bound Λ-S and Ω states, the spectroscopic constants, including the adiabatic excitation energy (T_e), equilibrium bond length (R_e), harmonic and anharmonic vibrational constants (ω_e and $\omega_e\chi_e$), and rotational constant (B_e, derived from the formula $B_v \approx B_e - (v + \frac{1}{2})\alpha_e$ with $v = 0$ and 1), are evaluated by the numerical solutions of the nuclear Schrödinger equations using Le Roy's LEVEL program.[21] The MR-CISD+Q dissociation energy (D_e) is obtained by subtracting the molecular energy at R_e from the energy at a large distance.

Results and Discussion

Before discussing the whole results in full detail, we will first investigate the performance of various methods on the spectroscopic constants of the ground state $X^2\Sigma^+$. In addition to MR-CISD+Q, single-reference methods of QCISD (quadratic configuration interaction with singles and doubles), QCISD(T) (QCISD with perturbative triples), CCSD (coupled-cluster with singles and doubles), and CCSD(T) (CCSD with perturbative triples) are also used. The results together with previous theoretical[14] and experimental[6,7] data are collected in Table 2 for comparison. First of all, the previous pseudopotential results[14] differ significantly from the present all-electron values at the same levels of theory. Noticeably, the effects of perturbative triple excitations revealed by comparing QCISD(T) with QCISD are also different in the two sets of calculations. All these may tentatively be ascribed to the limited flexibility in the basis sets used in the former calculations. It is well known that the calculation of the anharmonic vibrational constant $\omega_e\chi_e$ places great demanding on the theoretical methods. It is therefore not surprising that the calculated $\omega_e\chi_e$ values show fairly large deviations from each other. The large uncertainty in the experimental $\omega_e\chi_e$ values does not allow us to judge which theoretical calculation provides the most accurate $\omega_e\chi_e$. The experimental D_e of $InCl^+$ is not known so far. Here we derive an estimate of the D_e (0.65 eV) according to $D_0 + \omega_e/2$, where the D_0 of $InCl^+$ is estimated to be 0.63 eV from the D_0 of InCl (4.44 eV[22]) and the (adiabatic) ionization potentials of In and InCl (5.79,[23] 9.60 eV,[24] respectively). This estimated D_e together with the experimental R_e, ω_e, and B_e can now be used as guidelines to compare the theoretical calculations. The results by CCSD(T) and QCISD(T) are overall in best agreement with these experimental values among all the methods with the same basis set. However,

Table 2. Spectroscopic Constants of the $X^2\Sigma^+$ State: Comparison of Different Methods.

Methods	R_e (Å)	ω_e (cm^{-1})	$\omega_e\chi_e$ (cm^{-1})	B_e (cm^{-1})	D_e (eV)
This work					
MR-CISD[a]	2.323	338.7	6.70	0.117	0.36
MR-CISD[a,b]	2.277	346.2	7.15	0.121	0.38
MR-CISD+Q[a]	2.314	346.1	6.52	0.117	0.49
MR-CISD+Q[a,b]	2.275	356.5	3.59	0.122	0.56
QCISD	2.293	371.7	9.46	0.119	0.42
CCSD	2.292	366.6	9.87	0.119	0.40
QCISD(T)	2.304	335.4	5.45	0.118	0.52
CCSD(T)	2.301	339.3	5.93	0.118	0.50
Previous work[14]					
QCISD	2.270	347.0			
QCISD(T)	2.270	356.5			
Expt.					
6		354	4.9	0.117[c]	(0.65)[d]
7	2.303[e]	344.3	2.85		

[a]Using an active space consisting of nine electrons in eight orbitals (In $5s5p$ + Cl $3s3p$).

[b]Using the uncontracted ANO-RCC basis set.

[c]Estimated by the present authors from the experimental data with the formula $B_{v''} \approx B_e - (v'' + \frac{1}{2})\alpha_e$, where $v'' = 5$ and 6.

[d]Estimated value. See the discussion in the text.

[e]Fitted by the present authors from the RKR curves.

Table 3. The Effects of the BSSE and Variation of Electron Correlation on the Spectroscopic Constants[a] of $B^2\Sigma^+$ at the MR-CISD+Q Level.

Variation of electron correlation[b]		Without BSSE			With BSSE		
Inactive orbitals	Active orbitals	R_e (Å)	ω_e (cm^{-1})	D_e (eV)	R_e (Å)	ω_e (cm^{-1})	D_e (eV)
In 4*d*	In 5*s*5*p* + Cl 3*s*3*p*	2.587	327.4	2.64	2.590	327.3	2.62
In 4*d*	In 5*s*5*p*6*s* + Cl 3*s*3*p*	2.586	329.8	2.64	2.590	329.6	2.62
In 4*s*4*p*4*d*	In 5*s*5*p* + Cl 3*s*3*p*	2.585	329.1	2.66	2.590	329.0	2.63
In 4*s*4*p*4*d*	In 5*s*5*p*6*s* + Cl 3*s*3*p*	2.586	329.2	2.72	2.590	329.1	2.70
Using uncontracted ANO-RCC basis set:							
In 4*d*	In 5*s*5*p* + Cl 3*s*3*p*	2.493	384.3	2.33	2.497	383.1	2.30
In 4*d*	In 5*s*5*p*6*s* + Cl 3*s*3*p*	2.577	336.0	2.66	2.581	333.2	2.63

[a]Derived from polynomial fittings.
[b]Nine electrons in the active space. Inactive orbitals are those always doubly occupied.

they cannot be used with the uniform performance for all the states to be studied here, in particular, when the global PECs are explored. Actually, a few states of interest are multiconfigurational in nature even around the equilibria (see below), to which such single-reference methods do generally not apply. Moreover, the spin-orbit coupling cannot be accounted for at these levels of theory by MOLPRO. Therefore, we are confined to the MR-CISD method. The Davidson's correction (+Q) to MR-CISD for size-extensivity of correlation brings the results closer to the experiment values. Similar order of magnitude of such corrections is also observed for other states investigated here. At this stage we have to be concerned with the basis set effects. For this purpose additional calculations have been carried out with the uncontracted ANO-RCC (atomic natural orbital-relativistic correlation consistent) basis set (In: 22*s*19*p*13*d*5*f*3*g*, Cl: 17*s*12*p*5*d*4*f*2*g*).[25] The resultant R_e (2.275 Å) and ω_e (356.7 cm^{-1}) differ significantly from the corresponding values (2.314 Å, 246.1 cm^{-1}) obtained with the somewhat smaller basis set. At first glance one may draw a conclusion that the smaller basis set is insufficient. However, it turns out that this larger basis set has to be combined with a larger active space (e.g., In 5*s*5*p*6*s* + Cl 3*s*3*p*) in the MR-CISD+Q calculation. The R_e and ω_e then become 2.291 Å and 345.7 cm^{-1}, respectively, which are much closer to the results obtained with the smaller basis set. The same situation occurs also to other states. Instead, the results obtained with the smaller basis set are not sensitive to the size of the active space and number of correlated electrons, probably due to better error compensation. This is demonstrated in Table 3 by taking the $B^2\Sigma^+$ state as an example, where the basis set superposition errors (BSSEs) are also examined. Because the basis sets are uncontracted, the BSSEs are very small for all the properties. Until now, the stability of the MR-CISD+Q method has been established. Its results for $X^2\Sigma^+$ are quite satisfactory: The bond length (2.314 Å) differs from the experimental value (2.303 Å)[7] by only 0.01 Å, while the vibrational frequency of 346.1 cm^{-1} and the rotational constant of 0.117 cm^{-1} are in excellent agreement with the corresponding experimental data. As an additional piece of information, the calculated vertical and adiabatic ionization potentials of InCl are 9.45 and 9.35 eV, respectively, which are in good agreement with the experimental values of 9.71[5] and 9.60 eV.[24]

Having established the validation of the computational method, we now turn to discuss the whole results. The dissociation relationships for the possible low-lying Λ-S electronic states of $InCl^+$ are listed in Table 4, and the PECs of the corresponding doublet and quartet Λ-S states are shown in Figure 1. It can be seen that there are in total nine bound states, for which the fitted spectroscopic constants and the dominant configurations in the MCSCF wave functions are given in Table 5.

Both the $X^2\Sigma^+$ state and the $A^2\Pi$ state are correlated with the lowest dissociation limit of $In^+(^1S)$ + $Cl(^2P)$ (Fig. 1). The ground state $X^2\Sigma^+$ is characterized mainly by the configuration of $1\sigma^2 2\sigma^2 1\pi^4 3\sigma^1$, whereas $A^2\Pi$ by $1\sigma^2 2\sigma^2 1\pi^3 3\sigma^2$. In contrast to the bound $X^2\Sigma^+$ state, the $A^2\Pi$ state is essentially repulsive. Because of the crossing between the $A^2\Pi$ and $X^2\Sigma^+$ states, the presence of the spin-orbit coupling will change the PEC shape of the X1/2 state, a point to be discussed later in the present section.

There are 12 Λ-S excited states which dissociate to $In^+(^3P)$ + $Cl(^2P)$. The $B^2\Sigma^+$ state is the only one for which the high resolution experiment has been carried out.[6,7] The computed T_e = 26,686 cm^{-1}, ω_e = 328.5 cm^{-1}, and B_e = 0.094 cm^{-1} are in good agreement with the corresponding experimental values (T_e = 27,025 cm^{-1},[7] ω_e = 327.7 cm^{-1},[7] and B_e = 0.089 cm^{-1}[6]). However, the calculated bond length of 2.587 Å differs by 0.05 Å from the *estimated* experimental value of 2.638 Å, which is derived by the present authors from the RKR curves of ref. 7. As discussed above, the uncertainties inherent in the one-particle basis set and electron correlation treatment cannot explain such a large difference. Therefore, it is recommended that more accurate experimental measurements on the bond length of $B^2\Sigma^+$ should be carried out.

Table 4. Dissociation Relationships of the Low-Lying Λ-S States of $InCl^+$.

Atomic state (In^+ + Cl)	Λ-S states
$^1S + ^2P$	$^2\Sigma^+$, $^2\Pi$
$^3P + ^2P$	$^2\Sigma^+(2)$, $^2\Sigma^-$, $^2\Pi(2)$, $^2\Delta$, $^4\Sigma^+(2)$, $^4\Sigma^-$, $^4\Pi(2)$, $^4\Delta$

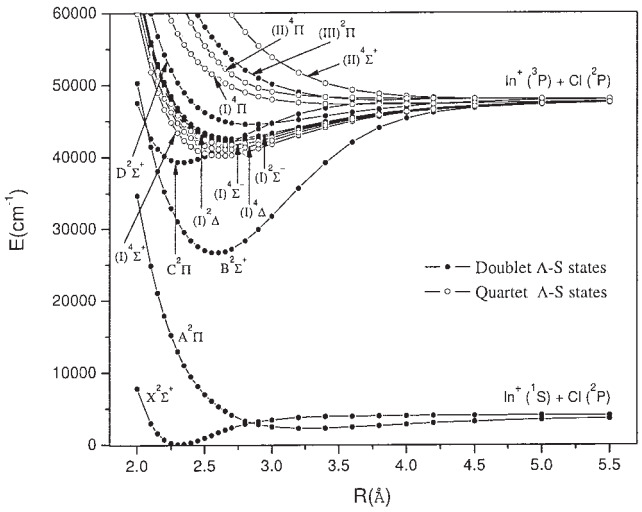

Figure 1. Potential energy curves of $InCl^+$: low-lying doublet and quartet Λ-S states.

The $C^2\Pi$ state has a deep potential well. The computed bond length and vibrational frequency are, respectively, 2.332 Å and 327.9 cm^{-1}. Its adiabatic excitation energy is calculated to be 39,290 cm^{-1}, being closer to that of the $C^2\Pi_{3/2}$ state (40,112 cm^{-1}) rather than that of the $C^2\Pi_{1/2}$ state (37,936 cm^{-1}).[8] This is because the scalar relativistic π orbital mimics more $\pi_{3/2}$ than $\pi_{1/2}$. The $C^2\Pi$ state tends to be predissociated because it crosses with five closely spaced excited states [i.e., $(I)^4\Sigma^+$, $(I)^4\Delta$, $(I)^4\Sigma^-$, $(I)^2\Delta$, and $(I)^2\Sigma^-$] arising from the same superconfiguration of $1\sigma^2 2\sigma^2 1\pi^3 3\sigma^1 2\pi^1$. This can be seen clearly from Figure 1. The $D^2\Sigma^+$ state as termed by Glenewinkel–Meyer et al.[8] is the third $^2\Sigma^+$ state of $InCl^+$. Its excitation energy has not been measured experimentally. However, a rough estimate may be induced according to the following observation: The $A^3\Pi_0^+$, $B^3\Pi_1$, and $C^1\Pi$ states of GaBr and InCl resulting from the valence iso-electronic configuration of $1\sigma^2 2\sigma^2 1\pi^4 3\sigma^1 2\pi^1$ have very similar excitation energies (GaBr: A 28,162 cm^{-1}, B 28,532 cm^{-1}, C 37,746 cm^{-1}; InCl: A 27,765 cm^{-1}, B 28,560 cm^{-1}, C 37484 cm^{-1}).[22,26] If the same situation occurs for the corresponding cations as well, the yet unknown experimental excitation energy of $InCl^+$ can then be estimated to be about 37,000 cm^{-1} by analogy with that of $GaBr^+$.[8] However, the computed excitation energy of 44,552 cm^{-1} is much larger than this estimate. A similar situation is also found in the case of $GaCl^+$: the experimental excitation energy of the $D^2\Sigma^+$ state is derived to be about 40,000 cm^{-1},[8] whereas the theoretical value is higher by 5000 cm^{-1}.[14] New experimental measurements are highly recommended to clarify these discrepancies. Above the $D^2\Sigma^+$ state, there are four repulsive states, namely $(I)^4\Pi$, $(III)^2\Pi$, $(II)^4\Pi$, and $(II)^4\Sigma^+$, among which the $(III)^2\Pi$ state corresponds to the unbound $E^2\Pi$ state as suggested by Glenewinkel–Meyer et al.[8]

In addition to the $B^2\Sigma^+ \rightarrow X^2\Sigma^+$ transition, Balfour and Chandrasekhar[6] also observed a red-degraded weak emission system of five bands between 320 and 335 nm, attributed to InCl or $InCl^+$. In our calculations, however, the proper transition cannot be identified. We believe this band system is relevant to some transition from a certain higher excited state, provided that it results from $InCl^+$.

Table 5. Spectroscopic Constants of the Low-Lying Λ-S States of $InCl^+$.

Λ-S state	T_e (cm^{-1})	R_e (Å)	ω_e (cm^{-1})	$\omega_e\chi_e$ (cm^{-1})	B_e (cm^{-1})	D_e (eV)	Dominant electronic configurations at R_e[a] (%)
$X^2\Sigma^+$	0	2.314	346.1	6.52	0.117	0.49	72.2 (A) + 10.0 (B)
Expt. 6	0		354	4.9	0.117[b]	(0.65)[c]	
7	0	2.303[d]	344.3	2.85			
$B^2\Sigma^+$	26,686	2.587	328.5	0.68	0.094	2.64	49.8 (B) + 13.9 (C) + 13.2 (A) + 5.1 (D)
Expt. 6	26,989[e]				0.089[f]		
7	27,205	2.638[d]	327.7	0.63			
$C^2\Pi$	39,290	2.332	327.9	2.59	0.127	1.08	61.9 (F) + 25.1 (G)
Expt. 8	Ω = 1/2: 37,936						
	Ω = 3/2: 40,112						
$(I)^4\Sigma^+$	40,180	2.624	232.8	1.88	0.100	0.97	89.0 (C)
$(I)^4\Delta$	41,037	2.657	221.8	1.95	0.098	0.86	89.3 (C)
$(I)^4\Sigma^-$	41,673	2.684	212.5	1.96	0.096	0.78	89.2 (C)
$(I)^2\Delta$	42,216	2.694	201.8	2.08	0.095	0.72	88.4 (C)
$(I)^2\Sigma^-$	42,539	2.702	197.2	2.07	0.094	0.68	88.4 (C)
$D^2\Sigma^+$	44,552	2.846	150.2	1.48	0.085	0.43	66.6 (C) + 8.1 (D) + 6.2 (E)

[a](A) $1\sigma^2 2\sigma^2 1\pi^4 3\sigma^1$; (B) $1\sigma^2 2\sigma^1 1\pi^4 3\sigma^2$; (C) $1\sigma^2 2\sigma^2 1\pi^3 3\sigma^1 2\pi^1$; (D) $1\sigma^2 2\sigma^1 1\pi^4 3\sigma^1 4\sigma^1$; (E) $1\sigma^2 2\sigma^2 1\pi^4 4\sigma^1$; (F) $1\sigma^2 2\sigma^2 1\pi^4 2\pi^1$; (H) $1\sigma^2 2\sigma^1 1\pi^4 3\sigma^1 2\pi^1$; weights lower than 5% are not reported.
[b]Estimated by the present authors from the experimental data with the formula $B_{v''} \approx B_e - (v'' + \frac{1}{2})\alpha_e$, where $v'' =$ 5 and 6.
[c]Estimated value. See the discussion in the text.
[d]Fitted by the present authors from the RKR curves.
[e]This value is v_{00}.
[f]This value is B_0.

Table 6. Dissociation Relationships and Energetics of Some Low-Lying Ω States of $InCl^+$.

Atomic state (In^+ + Cl)	Ω states	Energy (cm^{-1})		
		MR-CISD+Q[a]	MR-CISD+Q[b]	Expt. 27
$^1S_0 + {}^2P_{3/2}$	3/2, 1/2	0	0	0
$^1S_0 + {}^2P_{1/2}$	1/2	806	820	881
$^3P_0 + {}^2P_{3/2}$	3/2, 1/2	42,265	41,768	42,275
$^3P_0 + {}^2P_{1/2}$	1/2	43,071	42,588	43,156
$^3P_1 + {}^2P_{3/2}$	5/2, 3/2, 3/2, 1/2, 1/2, 1/2	43,223	42,975	43,349
$^3P_1 + {}^2P_{1/2}$	3/2, 1/2, 1/2	44,029	43,795	44,230
$^3P_2 + {}^2P_{3/2}$	7/2, 5/2, 5/2, 3/2, 3/2, 3/2, 1/2, 1/2, 1/2, 1/2	45,139	45,388	45,827
$^3P_2 + {}^2P_{1/2}$	5/2, 3/2, 3/2, 1/2, 1/2	45,945	46,208	46,708
Mean absolute error from experiment		278	412	

[a]Results obtained by diagonalizing $\langle\psi_I^{NR}|H_{BP} + E_{DKH}\delta_{IJ}|\psi_J^{NR}\rangle$.
[b]Results obtained by diagonalizing $\langle\psi_I^{DKH}|H_{BP}|\psi_J^{DKH}\rangle$.

The dissociation limits and corresponding energy separations for the possible low-lying Ω states are given in Table 6. Compared with Table 4, the dissociation limit $In^+(^1S)$ + $Cl(^2P)$ splits into two asymptotes when the spin-orbit coupling is taken into account, namely $^1S_0 + {}^2P_{3/2}$ and $^1S_0 + {}^2P_{1/2}$, while $In^+(^3P)$ + $Cl(^2P)$ into $^3P_0 + {}^2P_{3/2}$, $^3P_0 + {}^2P_{1/2}$, $^3P_1 + {}^2P_{3/2}$, $^3P_1 + {}^2P_{1/2}$, $^3P_2 + {}^2P_{3/2}$, and $^3P_2 + {}^2P_{1/2}$. Altogether there are 30 Ω states correlating with these eight asymptotes. As for the energetics, the state interaction approach amounts to diagonalizing the matrix $\langle\psi_I^{NR}|H_{BP} + E_{DKH}\delta_{IJ}|\psi_J^{NR}\rangle$, where ψ_I^{NR} standing for the nonrelativistic states of interest interacting via the spin-orbit operator. However, we find that the results obtained by diagonalizing $\langle\psi_I^{DKH}|H_{BP}|\psi_J^{DKH}\rangle >$ (ψ_I^{DKH} : scalar relativistic DKH wave function) are also in satisfactory agreement with experiment[27] (cf. Table 6). In this way, only one set (instead of two sets) of MCSCF and MR-CISD+Q calculations is necessary, leading to dramatic saving in the computational time. A better agreement between these two approaches could even be expected in the molecular calculations because the spin-orbit coupling is partially quenched. Therefore, all the calculations will be carried out with the latter method.

The PECs of 15 states of Ω = 1/2 and one state of Ω = 7/2 are plotted in Figure 2, while the other 10 states of Ω = 3/2 and four states of Ω = 5/2 are shown in Figure 3. The spectroscopic constants obtained by solving the nuclear Schrödinger equations are given in Table 7.

Although the ground Ω state, X1/2, has almost the same spectroscopic properties compared with the pure Λ-S ground state $X^2\Sigma^+$, the avoided intersection and the mixture between two Ω = 1/2 components (i.e. $X^2\Sigma^+_{1/2}$ and $A^2\Pi_{1/2}$) deform the PEC shape of the X1/2 state discernibly. Around the internuclear distance of 2.83 Å, the X1/2 state is composed of $X^2\Sigma^+_{1/2}$ and $A^2\Pi_{1/2}$ with almost equal weights. At shorter distances the former dominates, whereas at longer distances it is the latter that dominates. Only 11 bound vibrational levels ($v'' = 0$–10) of X1/2 are obtained in our calculations, implying that the $v'' > 10$ levels are dissociated as pointed out by Balfour et al.[6] We also notice that the A3/2 state intersects with X1/2 at about 2.84 Å with the crossing point very close to the $v'' = 10$ level. Therefore, the $v'' = 10$ level tends to be predissociated. According to Franck–Condon principle the X1/2 → A3/2 and A1/2 vertical transitions occur dominantly at the left and right inflexion points of the $v'' = 0$ level, if the heat distribution is neglected. Obviously, the transition energy at the right inflexion point (R = 2.381 Å) is lower (cf. Fig. 2). The computed lowest energy at which the vertical transitions start to occur is 9587 cm^{-1} for the X1/2 → A3/2 transition and 10,159 cm^{-1} for X1/2 → A1/2; being quite close to the observed value of about 9200 cm^{-1}.[5]

The spectroscopic constants of the B1/2 state are very close to those of $B^2\Sigma^+$, and are not affected by the avoided crossing point between the B1/2 and C1/2 states at about 2.1 Å. Two components of the $C^2\Pi$ state (C1/2 and C3/2) have been observed experimentally. The computed excitation energies are 38,283 and 40,336 cm^{-1}, respectively, which match well with the experimental values of 37,936 and 40,112 cm^{-1}.[8] The corresponding energy separation of 2053 cm^{-1} is in good agreement with the experimental value of 2175 ± 100 cm^{-1}.[8] The C3/2 state shows several avoided crossings with higher Ω = 3/2 states at about 2.4–2.7 Å, which renders two potential

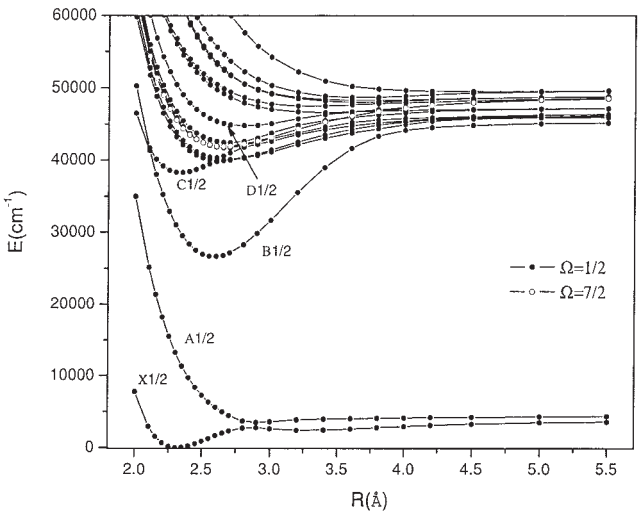

Figure 2. Potential energy curves of $InCl^+$: 15 Ω = 1/2 and one Ω = 7/2 states.

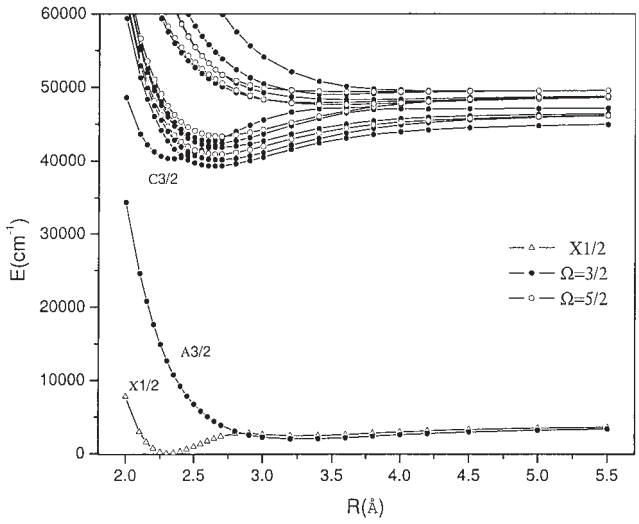

Figure 3. Potential energy curves of $InCl^+$: 10 Ω = 3/2 and four Ω = 5/2 states.

wells (cf. Fig. 3): the energetically lower one at a longer range (minimum at 2.645 Å) mainly results from the $(I)^4\Sigma^+$ state, which is denoted as C′3/2 in Table 7 and has not been observed experimentally. The energetically higher one is located at a shorter range (minimum at 2.336 Å) and arises from the $C^2\Pi$ state. The spin-orbit coupling causes a remarkable change to the shape of the PEC of the $D^2\Sigma^+$ state by mixing in $(I)^2\Sigma^-$, for example, the bond length of D1/2 is shorter by 0.037 Å than that of $D^2\Sigma^+$. The spin-orbit coupling also makes the PECs of the high-lying five closely spaced bound Λ-S states more complex. Their spectra have not been observed so that the degrees of agreement cannot be determined.

The radiative lifetime for a given vibrational level v' can be calculated by the following formula:[28,29]

$$\tau_{v'} = (A_{v'})^{-1} = \frac{3h}{64\pi^4 |a_0 \cdot e \cdot \overline{TDM}|^2 \sum_{v''} q_{v',v''} (\Delta E_{v',v''})^3} \cdot \frac{g'}{g''}$$

$$= \frac{4.936 \times 10^5}{|\overline{TDM}|^2 \sum_{v''} q_{v',v''} (\Delta E_{v',v''})^3} \cdot \frac{g'}{g''}$$

where $q_{v',v''}$ is the Franck–Condon factor, $\overline{TDM}$ is the averaged transition dipole moments (TDM) in atomic unit, g' and g'' are, respectively, the degeneracy of the upper and lower states (equal to 2 in this case), the energy difference $\Delta E_{v',v''}$ is in cm^{-1}, and $\tau_{v'}$ is in s. The TDMs of 17 transitions are plotted in Figure 4 as a function of the internuclear distance. In the Franck–Condon region, the B1/2–, C1/2–, C3/2–, and D1/2–X1/2 transitions have much larger transition moments than the other 13 transitions and thus have shorter radiative lifetimes. For the lowest four vibrational levels of selected transitions,

Table 7. Spectroscopic Constants of the Low-Lying Ω States of $InCl^+$.

Ω state	T_e (cm^{-1})	R_e (Å)	ω_e (cm^{-1})	$\omega_e\chi_e$ (cm^{-1})	B_e (cm^{-1})	D_e (eV)	Dominant Λ-S states at R_e (%)
X1/2	0	2.314	343.9	6.06	0.117	0.44	99.9 ($x^2\Sigma^+$)
Expt. 6	0		354	4.9	0.117[a]	(0.65)[b]	
7	0	2.303[c]	344.3	2.85			
B1/2	26,650	2.588	328.2	0.61	0.094	2.30	99.6 ($B^2\Sigma^+$)
Expt. 6	26,989[d]				0.089[e]		
7	27,025	2.638[c]	327.7	0.63			
C1/2	38,283	2.332	323.9	0.70	0.127	0.95	99.5 ($C^2\Pi$)
Expt. 8	37,936						
C′3/2	39,321	2.645	205.1	1.42	0.099	0.70	73.9 ($(I)^4\Sigma^+$) + 24.8 ($(I)^4\Sigma^-$)
(V)1/2	39,984	2.616	228.5	2.24	0.101	0.77	74.8 ($(I)^4\Sigma^+$) + 15.9 ($(I)^4\Delta$)
(III)3/2	40,165	2.682	200.9	2.59	0.096	0.74	67.1 ($(I)^4\Delta$) + 30.4 ($(I)^2\Delta$)
C3/2	40,336	2.336	321.8	0.47	0.126	0.58	99.5 ($C^2\Pi$)
Expt. 8	40,112						
(VI)1/2	40,369	2.589	389.3	12.94	0.104	0.75	67.5 ($(I)^4\Delta$) + 25.8 ($(I)^4\Sigma^+$) + 5.3 ($C^2\Pi$)
(I)5/2	40,924	2.668	213.6	2.07	0.097	0.65	84.5 ($(I)^4\Delta$) + 14.3 ($(I)^2\Delta$)
(VII)1/2	41,745	2.679	242.8	3.97	0.097	0.58	87.8 ($(I)^4\Sigma^-$) + 8.2 ($(I)^4\Sigma^+$)
(IV)3/2	41,867	2.706	211.2	2.76	0.095	0.56	67.2 ($(I)^2\Delta$) + 29.9 ($(I)^4\Delta$)
(I)7/2	41,887	2.654	232.0	2.58	0.098	0.83	100 ($(I)^4\Delta$)
(V)3/2	42,081	2.606	296.5	7.11	0.102	0.63	54.3 ($(I)^2\Delta$) + 24.3 ($(I)^4\Delta$) + 16.8 ($C^2\Pi$)
(VIII)1/2	42,426	2.705	235.3	1.82	0.095	0.59	90.0 ($(I)^2\Sigma^-$)
(VI)3/2	42,699	2.612	350.2	5.99	0.102	0.73	66.2 ($(I)^4\Sigma^-$) + 23.2 ($(I)^4\Sigma^+$) + 10.1 ($C^2\Pi$)
(II)5/2	43,355	2.683	213.7	2.56	0.096	0.65	84.9 ($(I)^2\Delta$) + 14.7 ($(I)^4\Delta$)
D1/2	44,819	2.809	169.8	1.71	0.087	0.29	87.9 ($D^2\Sigma^+$) + 6.5 ($(I)^2\Sigma^-$)

[a]Estimated by the present authors from the experimental data with the formula $B_{v''} \approx B_e - (v'' + \frac{1}{2})\alpha_e$, where $v'' = 5$ and 6.
[b]Estimated value. See the discussion in the text.
[c]Fitted by the present authors from the RKR curves.
[d]This value is v_{00}.
[e]This value is B_0.

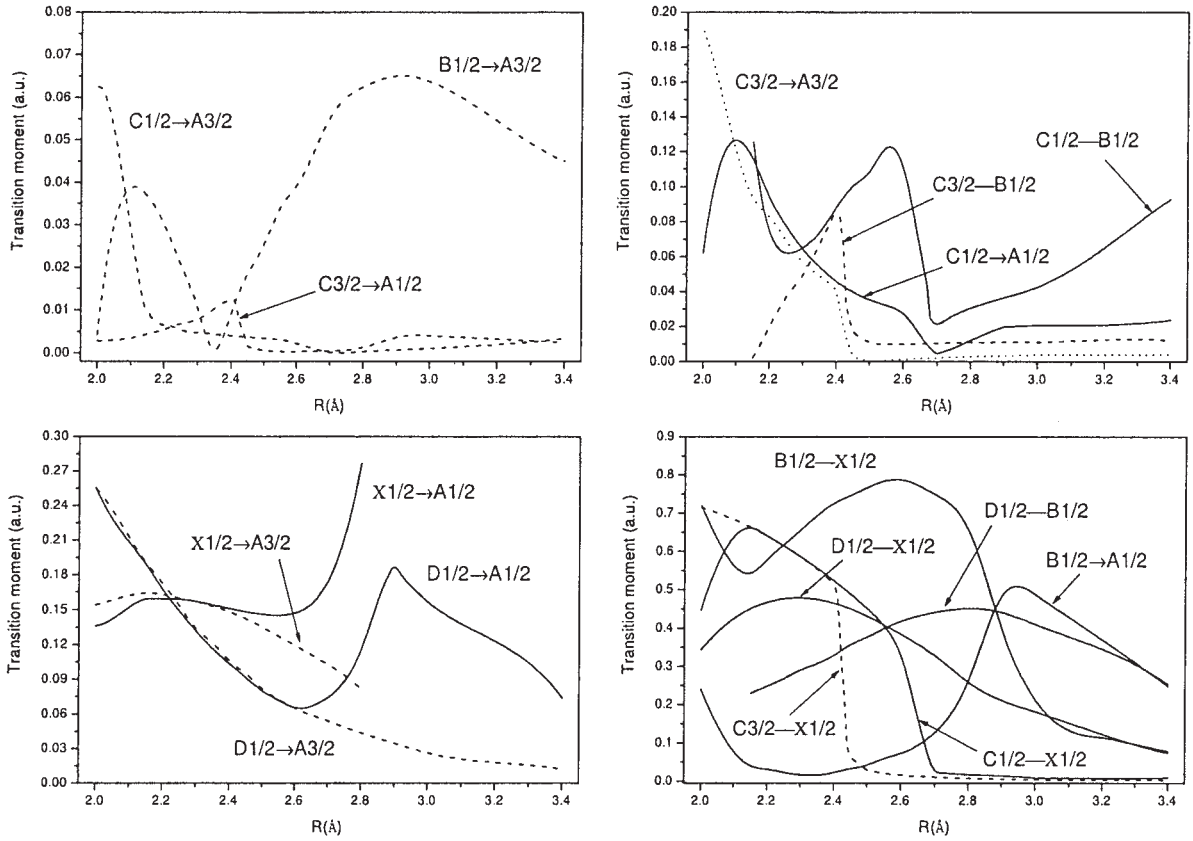

Figure 4. Transition dipole moments as a function of internuclear distance. Solid, dashed, and dotted lines are for the transitions between 1/2 and 1/2, 1/2 and 3/2, and 3/2 and 3/2, respectively.

we have tabulated the radiative lifetimes in Table 8 and the Franck–Condon factors in Table 9. As expected, the aforementioned four transitions are remarkably strong with the lifetimes being of the order of nanoseconds. On the other hand, the other transitions are rather weak, because not only do the transitions between excited states have smaller TDMs, but they also have smaller energy separations. Close inspections reveal that, at the lowest vibrational level ($v' = 0$), the C1/2– and C3/2–X1/2 transitions mainly come from the 0–0 band. For the B1/2–X1/2 transition, which has no dominant band, the lifetime of 49.2 ns is the weighted average of several bands. The lifetime is also affected by the Franck–Condon factor. In the case of the D1/2–X1/2 transition, for example, the relatively long lifetime of 194.4 ns is owing to the small Franck–Condon factors (summed up about 0.54), despite its large TDM and energy separations.

Table 8. Radiative Lifetimes of Transitions at Different Vibrational Levels.

	Radiative lifetimes			
Transition	$v' = 0$	$v' = 1$	$v' = 2$	$v' = 3$
B1/2–X1/2	49.2 ns	50.0 ns	50.2 ns	57.1 ns
C1/2–X1/2	27.7 ns	28.2 ns	28.8 ns	29.4 ns
C1/2–B1/2	157.0 μs	125.3 μs	110.3 μs	84.6 μs
C3/2–X1/2	24.2 ns			
C3/2–B1/2	100.2 μs			
D1/2–X1/2	194.4 ns	276.8 ns	378.3 ns	369.4 ns
D1/2–B1/2	562.6 ns	586.5 ns	610.4 ns	634.0 ns

ns: nanosecond; μs: microsecond.

Conclusions

Extensive *ab initio* all-electron relativistic calculations on the ground and low-lying excited states of $InCl^+$ have been performed. Based on the potential energy curves the spectroscopic constants of the bound Λ-S and Ω states are derived by solving the corresponding nuclear Schrödinger equations, and found to be in good agreement with the available experimental values. However, new experiments should be carried out to resolve the remaining discrepancies. The bound lengths and vibrational constants of the X1/2, B1/2, C1/2, and C3/2 states differ very little from their corresponding Λ-S states. However, the spin-orbit coupling has significant effects on the dissociation energies and the shape of the PECs in the presence of avoided

Table 9. Theoretical Franck–Condon Factors of Selected Transitions.

	$v'' = 0$	1	2	3	4	5	6	7	8	9	10
B1/2–X1/2											
$v' = 0$	0.0002	0.0025	0.0185	0.0767	0.1945	0.3030	0.2750	0.1172	0.0100	0.0015	0.0004
1	0.0010	0.0118	0.0574	0.1350	0.1350	0.0187	0.0695	0.3167	0.2287	0.0110	0.0108
2	0.0034	0.0301	0.0960	0.1164	0.0230	0.0297	0.0901	0.0009	0.2824	0.2813	0.0007
3	0.0085	0.0546	0.1087	0.0512	0.0052	0.0767	0.0106	0.0482	0.0026	0.2898	0.1541
C1/2–X1/2											
$v' = 0$	0.9610	0.0390	0.0000	0.0000	0.0000	0.0000	0.0000	0.0000	0.0000	0.0000	0.0000
1	0.0367	0.8956	0.0676	0.0000	0.0001	0.0000	0.0000	0.0000	0.0000	0.0000	0.0000
2	0.0022	0.0593	0.8516	0.0864	0.0002	0.0002	0.0000	0.0000	0.0000	0.0000	0.0000
3	0.0001	0.0058	0.0697	0.8253	0.0980	0.0010	0.0001	0.0001	0.0000	0.0000	0.0000
C3/2–X1/2											
$v' = 0$	0.9450	0.0547	0.0003	0.0001	0.0000	0.0000	0.0000	0.0000	0.0000	0.0000	0.0000
D1/2–X1/2											
$v' = 0$	0.0000	0.0000	0.0000	0.0000	0.0001	0.0006	0.0036	0.0182	0.0719	0.1865	0.2592
1	0.0000	0.0000	0.0000	0.0001	0.0005	0.0033	0.0154	0.0544	0.1294	0.1500	0.0365
2	0.0000	0.0000	0.0000	0.0003	0.0020	0.0100	0.0354	0.0845	0.1065	0.0257	0.0277
3	0.0000	0.0000	0.0001	0.0009	0.0055	0.0217	0.0573	0.0880	0.0449	0.0044	0.0859

crossings. The potential well of the ground state (X1/2) is found to consist of 11 bound vibrational levels ($v'' = 0–10$).

The present calculations reveal that, the B1/2–, C1/2–, C3/2–, and D1/2–X transitions in the Franck–Condon region are rather strong. These excited states are short lived, with the radiative lifetimes in the range of 20–200 ns.

Acknowledgments

The authors are grateful to the unknown referees for helpful suggestions.

References

1. Donnelly, V. M.; Karlicek, R. F. J Appl Phys 1982, 53, 6399.
2. Karlicek, R. F.; Hammarlund, B.; Ginocchio, J. J Appl Phys 1986, 60, 794.
3. Zou, W.; Lin, M.; Yang, X.; Zhang, B. J Chem Phys 2003, 119, 3721.
4. Berkowitz, J.; Dehmer, J. L. J Chem Phys 1972, 57, 3194.
5. Egdell, R. G.; Orchard, A. F. J Chem Soc Faraday Trans II 1978, 74, 1179.
6. Balfour, W. J.; Chandrasekhar, K. S. J Mol Spectrosc 1987, 124, 443.
7. Balfour, W. J.; Chandrasekhar, K. S.; Saksena, M. D. J Mol Spectrosc 1991, 145, 458.
8. Glenewinkel–Meyer, T.; Kowalski, A.; Müller, B.; Ottinger, C.; Breckenridge, W. H. J Chem Phys 1988, 89, 7112.
9. Nampoori, V. P. N.; Patel, M. M. Curr Sci 1979, 48, 12.
10. Perumalsamy, K.; Rai, S. B.; Upadhya, K. N.; Rai, D. K. Phisica C 1985, 132, 122.
11. Kim, G.-S.; Hirst, D. M. Mol Phys 1997, 90, 43.
12. Glenewinkel–Meyer, T.; Müller, B.; Ottinger, C.; Rosmus, P.; Knowles, P. J.; Werner, H.-J. J Chem Phys 1991, 95, 5133.
13. Yoshikawa, M.; Hirst, D. M. Chem Phys Lett 1995, 244, 258.
14. Schwerdtfeger, P.; Fischer, T.; Dolg, M.; Igel–Mann, G.; Nicklass, A.; Stoll, H.; Haaland, A. J Chem Phys 1995, 102, 2050.
15. MOLPRO, a package of ab initio programs designed by Werner, H.-J.; Knowles, P. J. Version 2002.7, with contributions from Amos, R. D.; Bernhardsson, A.; Berning, A.; Celani, P.; Cooper, D. L.; Deegan, M. J. O.; Dobbyn, A. J.; Eckert, F.; Hampel, C.; Hetzer, G.; Knowles, P. J.; Korona, T.; Lindh, R.; Lloyd, A. W.; McNicholas, S. J.; Manby, F. R.; Meyer, W.; Mura, M. E.; Nicklass, A.; Palmieri, P.; Pitzer, R.; Rauhut, G.; Schütz, M.; Schumann, U.; Stoll, H.; Stone, A. J.; Tarroni, R.; Thorsteinsson, T.; Werner, H.-J.
16. Dyall, K. G. Theor Chem Acc 1998, 99, 366, and reoptimized by de Jong, W.
17. Woon, D. E.; Dunning, T. H., Jr. J Chem Phys 1993, 98, 1358.
18. Douglas, M.; Kroll, N. M. Ann Phys 1974, 82, 89.
19. Hess, B. A. Phys Rev A 1986, 33, 3742.
20. Berning, A.; Schweizer, M.; Werner, H.-J.; Knowles, P. J.; Palmieri, P. Mol Phys 2000, 98, 1823.
21. Le Roy, R. J. LEVEL 7.4: A Computer Program for Solving the Radial Schrödinger Equation for Bound and Quasibound Levels; University of Waterloo: Chemical Physics Research Report CP-642R3, 2001.
22. Huber, K. P.; Herzberg, G. Molecular Spectra and Molecular Structure IV: Constants of Diatomic Molecules; Van Nostrand-Reinhold: New York, 1979.
23. Dönszelmann, A.; Neijzen, J. H. M. Acta Phys Pol A 1983, 63, 201.
24. Johnson, R. D., III; Dearden, D. V.; Hudgens, J. W. J Chem Phys 1994, 100, 3422.
25. Roos, B. O.; Lindh, R.; Malmqvist, P.-A.; Veryazov, V.; Widmark, P.-O. J Phys Chem A 2004, 108, 2851.
26. Yang, X.; Lin, M.; Zhang, B. J Phys Chem A 2004, 108, 4341.
27. Moore, C. E. Atomic Energy Levels; National Bureau of Standards: Washington, DC, 1971.
28. Okabe, H. Photochemistry of Small Molecules; Wiley–Interscience: New York, 1978.
29. Heaven, M. C. Chem Soc Rev 1986, 15, 405.